INFLUENCE OF PARAMETERIZATION AND OPTIMIZATION METHOD ON THE OPTIMUM AIRFOIL

B.G. MARINUS
Royal Military Academy/von Karman Institute for Fluid Dynamics, Brussels/Sint-Genesius-Rhode, Belgium

Keywords: *airfoil, parameterization, optimization, aerodynamics*

Abstract

The potential influence of different combinations of parameterization methods and optimization strategies on the attainable optimum and the optimization cost is evaluated by comparisons of the optimized airfoils. The optimization strategies consist of a single-objective metamodel assisted Genetic Algorithm and multi-objective Differential Evolution both assisted and non-assisted. B-spline and Bézier formulations are used together with a direct and standard description of the airfoil shape. The multi-point optimizations are applied to airfoils in 2D cascades corresponding to propeller geometries.

Nomenclature

$B_{i,q}(.)$	Basis function
c	Airfoil chord
$\overline{C}(.)$	Curve coordinate vector
C_d	Airfoil drag coefficient
C_l	Airfoil lift coefficient
C_p	Pressure coefficient
$\overline{dD}$	Elemental drag
$\overline{dL}$	Elemental lift
$\overline{dT}$	Elemental thrust
$\overline{dU}$	Elemental torque force
f_1, f_2	Weighting factor
J	Advance ratio
M_∞	Free-stream Mach number
n, N, q	Variables
r	Radius
R_{tip}	Propeller tip radius
u	Running coordinate
v_∞	Free-stream velocity
$w_.$	Weight
$\overline{X}$	Coordinate vector
α	Local angle of attack
β	Local blade angle
ε, γ	Angle
η_{el}	Elemental efficiency
Σ	Overall performance
τ	Constraint penalty
$\Omega_.$	Objective function
ω	Angular velocity
ρ	Air specific mass

Abreviations

ANN	Artificial Neural Network
DOE	Design Of Experiments
GA	Genetic Algorithm
MODE	Multi-Objective Differential Evolution
RANS	Reynolds Averaged Navier-Stokes

1 Introduction

The airfoils selected to shape propeller blades are of primary importance. The key role in transforming the engineering problem of optimizing an airfoil shape in a mathematical problem lies within the parameterization technique used to represent the airfoil. Most works in airfoil optimization, ranging from pure aerodynamic to multidisciplinary optimization for turbomachinery applications or wings, rely on spline

parameterization [1, 2, 3, 4, 5, 6, 7, 8] or Bézier parameterization [9, 10, 11, 12, 13, 14, 15] with typically 10 to 50 parameters. Unfortunately, few papers assess the influence of the parameterization technique [16, 17, 18, 19], in particular b-spline versus Bézier parameterization. Moreover, the influence of the combination of a parameterization with an optimization technique is seldom analyzed [20, 21]. For these reasons, the present effort investigates the effect of both the blade parameterization and optimization technique on the attainable optimum and on the computational cost of the process. Comparisons are made in a realistic multidisciplinary optimization environment for complex engineering applications with a moderate total number of design variables -$O(30 \sim 40)$- so that only a limited amount of parameters (< 10) are dedicated to the airfoil shape for the remaining parameters are assigned to other design variables such as radial distributions of sweep, twist, thickness and chord in the case of propellers.

2 Airfoil shape parameterizations

The b-spline and Bézier representations have been selected among the various formulations available for the designer because they are a flexible technique, providing smooth shapes with few design parameters. Both are based on a set of control points that define the shape of the curve and the convex hull of the control polygon, formed by joining neighboring control points, contains the curve. This implies that the design parameters (i.e. the position of the control points) control important features of the design problem and explains their popularity for optimization purposes.

Bézier and b-spline representations rely on a set of $n+1$ control points $\overline{X_0}$, $\overline{X_1}$,...,$\overline{X_n}$ and the expression of the curve $\overline{C}(u)$ is given in both cases by:

$$\overline{C}(u) = \sum_{i=0}^{n} B_{i,q}(u)\overline{X_i} \qquad (1)$$

over the interval $u \in [0,1]$ with q computed from the required degree of the curve in order to achieve the desired continuity properties. They differ by the basis functions used to compute the $B_{i,q}(u)$ coefficients. Bézier curves with $n+1$ control points are of degree $q = n$ whereas b-spline curves require a more complex theory with more information (i.e. the degree of the curve q must be chosen and a knot vector comprising $n+q+1$ elements must be defined over the same interval with multiplicity of the $q+1$ first and last elements to define a clamped b-spline). This disadvantage is compensated by the fact that b-splines have the local modification property together with all important properties of Bézier curves such as the convex hull property and at least $\mathcal{C}^2$-continuity if the number of control points $n+1$ is chosen accordingly. The local modification property implies that changing a control point does not globally change the shape of the curve and allows a more localized shape control. This interesting property [19] is illustrated on figure 1 where curves for both representations are drawn for two sets of control points differing only in the y-coordinate of one single point. Irrespectively of the difference in shape due to the particular formulation, the local character of the modification is clearly illustrated by the absence of any impact of the change of a single parameter on the trailing part of the curve.

In combination with the previous two formulations, two approaches to describe the airfoil shape were investigated . The first one has the control points directly controlling the shape of the entire airfoil as in [22, 23] and [7]. As shown on figure 2, this *direct* parameterization uses 7 control points for the suction side and 6 points for the pressure side. This results in only 9 parameters because the leading edge and trailing edge locations are fixed and $\mathcal{C}^2$-continuity is ensured at these locations through a careful handling of endpoint curvature by clamping the relative position of the first and last two control points on the pressure-side with respect to the control points on the suction-side as is suggested on figure 2. This leaves only 2 parameters con-

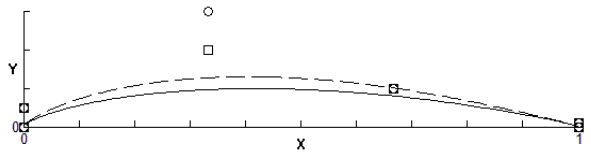

(a) Bézier parameterization.

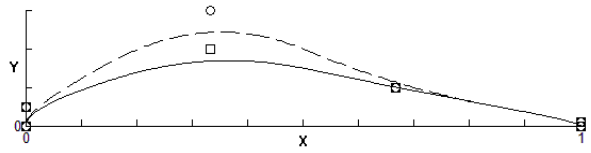

(b) B-spline parameterization.

Fig. 1 Local modification property illustrated with two sets of control points differing only in a single coordinate (□ and — or ○ and – –).

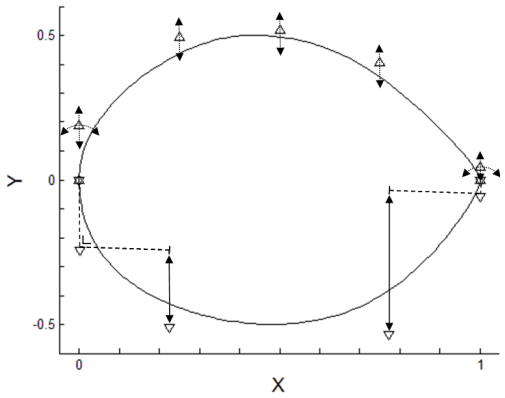

Fig. 2 Direct parameterization and degrees of freedom for the control points .

trolling the ordinate difference between the third and fourth control points on the pressure-side.

The second approach consists of a thickness distribution that is set upon a camberline in the way proposed by Abbott et al [24]. This *standard* NACA-type parameterization is illustrated on figure 3. It uses 6 control points with 6 parameters to control the shape of the thickness distribution and 4 additional points with 2 parameters to control the shape of the camberline. Although the direct parameterization has inherently more freedom to generate radical new shapes than the standard one, it is expected to be less suitable to produce efficient designs precisely because of the larger search space in terms of shape [19]. Indeed, for a comparable search space in terms of parameters, the *direct* parameterization delivers more non airfoil-like shapes even if the parameters are chosen such that a minimum thickness is guaranteed. Moreover, the standard description, on top of its intrinsic capability of delivering airfoil-like shapes, has demonstrated its efficiency [16, 25] thanks to a close relationship between the aerodynamic behavior and the thickness and camber distributions.

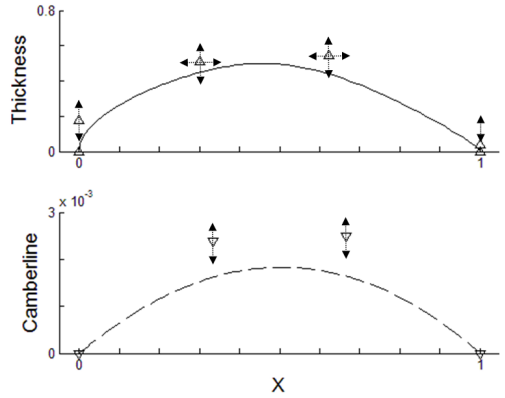

(a) Thickness and camberline distributions with control points and their respective degrees of freedom.

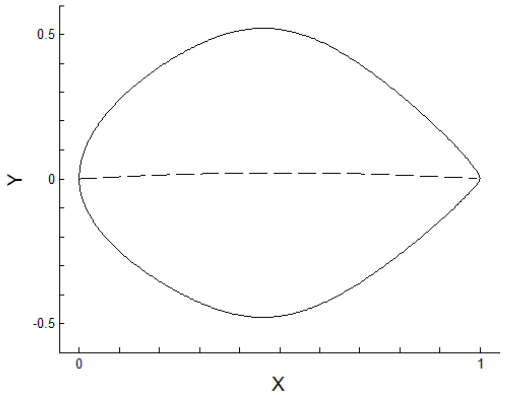

(b) Airfoil shape and camberline.

Fig. 3 Standard parameterization and degrees of freedom for the control points.

3 Elemental efficiency

The airfoil obtained by one of the parameterizations is used to define a propeller blade (figure 4(a)) with a prescribed radial distribution of chord, thickness and twist. The chord and thickness are constant up to 80% radius and the blade has no sweep. From blade element theory, it is easily shown that the efficiency of a blade element (see figure 4(b)) that produces the elemental thrust $\overline{dT}$ and the elemental torque force $\overline{dU}$, is given by:

$$\eta_{el} = \frac{\tan\gamma}{\tan(\gamma+\varepsilon)} \tag{2}$$

where

$$\gamma = \arctan\frac{v_\infty}{\omega r} = \arctan\frac{JR_{tip}}{\pi r}$$

and

$$\varepsilon = \arctan\frac{|\overline{dD}|}{|\overline{dL}|} \tag{3}$$

Equations 2 and 3 reveal the importance of increasing the lift-to-drag ratio $|\overline{dL}|/|\overline{dD}|$ of all blade elements in order to achieve better overall efficiency. Note that as the twist distribution is prescribed, so is also the angle of attack $\alpha(r) = \beta(r) - \gamma(r)$ of the airfoil. The engineering problem of finding the optimum airfoil shape under transonic conditions at $M_\infty = 0.75$ with a constant advance ratio $J = 3.3$, is simplified by optimizing one single airfoil for three radii (50%, 75% and 97.5%). Each radius defines a 2D high pitch cascade at fixed angle of attack as shown on figure 4. The objective of the optimization is to reduce C_d and $1/C_l$ concurrently for the three cascades.

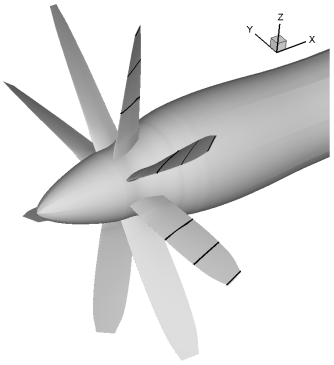

(a) View of the three radii (50%, 75% and 97.5%) chosen for the multi-point optimization of the airfoil in the corresponding blade passage.

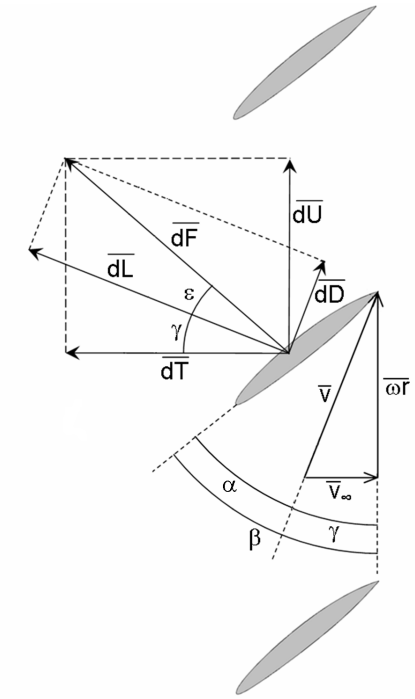

(b) 2D geometry of a blade passage at given radius r.

Fig. 4 Airfoil cascade geometry.

4 Optimization techniques and objectives

Evolutionary methods have excellent robustness and a high potential to find the global optimum of complex problems involving a large number of design parameters associated with a discontinuous and non-convex objective domain

[26, 20, 27]. Two techniques have been investigated for the present multi-point optimization: a single-objective binary-coded Genetic Algorithm (GA) and Multi-Objective Differential Evolution (MODE).

The binary-coded GA [28, 29] closely mimics natural evolution by coding the parameters of an individual (i.e. a blade design) in a binary string or genotype. The genotype translates into a particular shape (the phenotype), and its performance is evaluated. Members of a generation are obtained through reproduction of two parents selected by a tournament in which only the best of any combination of two individuals is retained. The reproduction mechanism consists of an exchange of parts from their genotype through crossover. Then a mutation operator changes a random bit in the binary string of the offspring. Ultimately elitism is applied as the best individual from the parent population is carried over if it outperforms all offspring. The selection procedure relies on performance estimates cast into an aggregated objective Ω_{GA} to be minimized. It is computed by the weighted sum of performance estimates for the three radii:

$$\Omega_{GA} = \sum_{i=1}^{3} w_i (f_1 C_{d,i} + f_2 \frac{1}{C_{l,i}}) + \tau \qquad (4)$$

where the weights w_i are chosen such that the 75% radius section has twice more impact on the optimization result and the factors f_1 and f_2 ensure that a drag reduction or a lift increase affect the objective value in a comparable way. τ is an external penalty triggered only if the airfoil has insufficient thickness so that the feasability of the design is ensured. The estimates are provided by an Artificial Neural Network (ANN). The purpose of this model is to reduce the computational cost so that the evolutionary process can be spread over a large amount of generations. The ANN is trained using a database of RANS simulations initially obtained for geometries defined by a Design Of Experiments (DOE). The purpose of the DOE is to fill the search space with carefully selected samples to allow extraction of maximum information about the underlying input-output relationships. The accuracy of the surrogate model is improved during the evolutionary process by recursive training of the ANN each time the database is augmented with the most promising individual of every 1000 generations. The process is repeated for 100 iterations using each time the new ANN for 1000 generations comprising each 50 individuals (see figure 5).

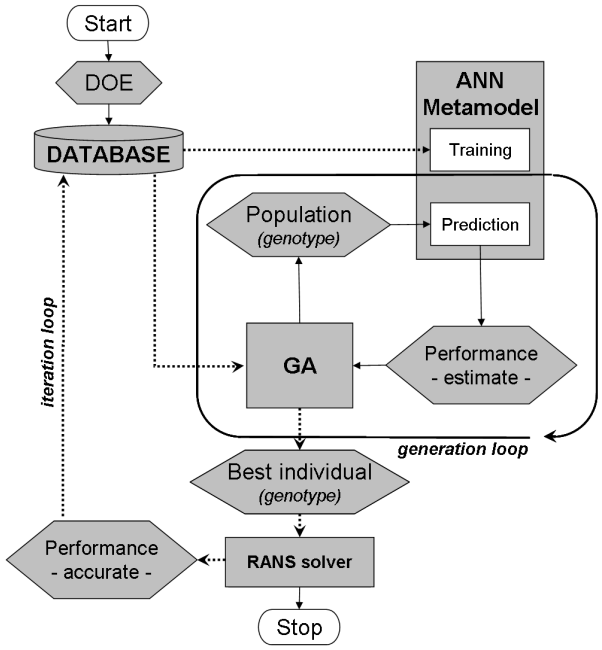

Fig. 5 Layout of the single objective binary coded GA-optimizer with its metamodel.

Differential Evolution has been developed by Price and Storn [30] and does not require parameters to be coded in a binary string. A new generation of N individuals is formed by mutation and recombination among the N parents. Indeed, the vector of parameters of an offspring is a recombination of parameters that are randomly chosen either from one parent or from a linear combination of parameters from three other individuals chosen randomly in the Pareto front. This last step is also responsible for mutation. Multi-objective selection is performed in the way proposed by Madavan [31] through Pareto ranking of parent and child populations together with respect to the two

objectives to be minimized:

$$\begin{cases} \Omega_1 = \sum_{i=1}^{3} w_i C_{d,i} \\ \Omega_2 = \sum_{i=1}^{3} w_i \frac{1}{C_{l,i}} \end{cases} \quad (5)$$

in which the weights w_i have the same value as for the GA. Note that with this approach, the trouble of choosing adequately the f factors is relieved and the external penalty on thickness is dealt with by a separate constraint function. The population size for the next evolutionary step is restored to its original size because only the N best ranked individuals are passed while also looking after the diversity of the population by rejecting individuals with a too high degree of similarity. With respect to performance assessment, two cases have been considered: a two-level case in which the performance is assessed through an ANN-metamodel that is trained with RANS simulations every 1000 generations (figure 6(a)), and a single-level case for which only accurate RANS simulations are used (figure 6(b)). The first approach is highly similar to the one used for the GA with the difference that now the whole population of N individuals is passed through the iteration loop and hence analyzed by the RANS solver, as suggested on figure 6. The second approach consists of a single generation loop and as no metamodel is used, it offers the advantage that it is not subject to the inaccuracy of the performance estimates. However, less generations (100) are considered in this case because of the elevated numerical cost associated with the RANS evaluation of the complete generation. Nevertheless, it provides a convenient comparison to assess the effect of the metamodel. The population size for both approaches is 20 and the individual RANS simulations can be performed concurrently.

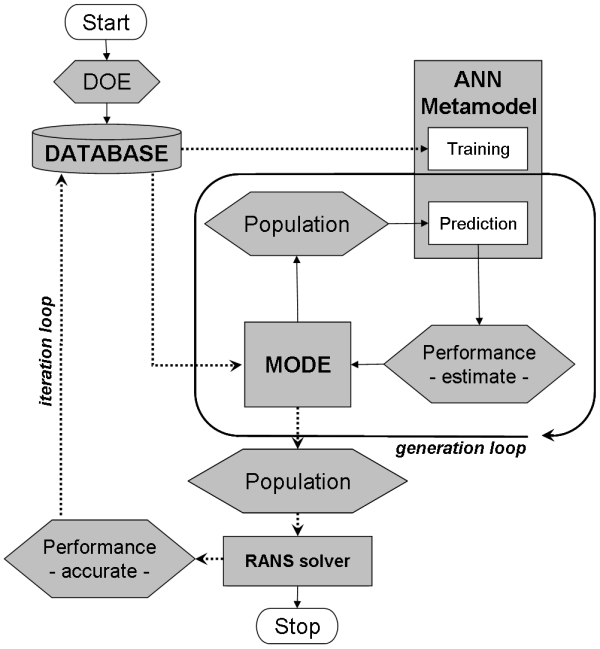

(a) Two level approach.

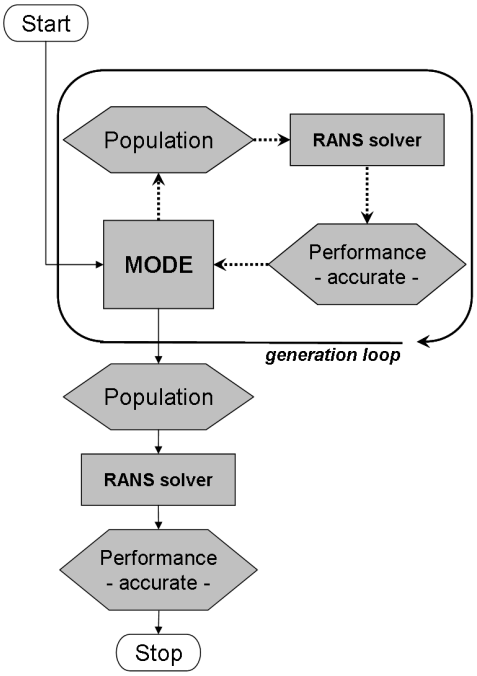

(b) Single level approach.

Fig. 6 Layout of the single and two-level MODE-optimizers.

5 Results

The RANS simulations are performed by means of the *TRAF 2D* solver for transonic flow [32]. It uses a multi-stage Runge-Kutta time integration in conjunction with acceleration techniques

on a H-type mesh with 100 grid-points on the suction and pressure-side and 96 points in the wall-normal direction. The equations are discretized using a cell-centered finite volume scheme with artificial dissipation of the Jameson type. Acceleration techniques comprise local time stepping, variable coefficient implicit residual smoothing and a full multigrid method. The effect of turbulence is accounted for by the eddy-viscosity hypothesis expressed through the two-layer mixing length model of Baldwin and Lomax. A NACA 16-009 airfoil is used as benchmark because it is commonly used for propellers.

Table 1 gives an overview of the different cases together with the number of iterations necessary to reach the optimum. Despite converging early toward their respective optimum, all optimizations were ran for 100 iterations (or generations in the MODE single level case) in order to ensure that absolute convergence is reached. For cases F, G and J, no solution better than the benchmark was found after 100 iterations in spite of modifications to the evolutionary and metamodel settings. For these cases, the optimization is considered as not having succeeded. These non-optimum airfoils are shown as well for completeness. In each case where the metamodel is used, the database has 64 samples thereby requiring 192 calls to the RANS solver. Disregarding the parameterization type, all optimizations have an identical search domain as each parameter is allowed to fluctuate over the same interval in all cases. The overall performance of an airfoil is measured by its Σ-value (given in table 1) which is the mass-flow averaged area under the C_l/C_d curve normalized by the corresponding area for the benchmark:

$$\Sigma = \frac{\int_{R_{root}}^{R_{tip}} 2\pi\rho_\infty v(r) \left.\frac{C_l(r)}{C_d(r)}\right|_{\text{airfoil}} rdr}{\int_{R_{root}}^{R_{tip}} 2\pi\rho_\infty v(r) \left.\frac{C_l(r)}{C_d(r)}\right|_{\text{NACA 16-009}} rdr} \quad (6)$$

The purpose of mass-flow averaging in the Σ-value is to yield a fair overall performance that takes the radial distribution of the mass-flow, hence the radial distribution of the load, into account. Nevertheless, the Σ-values clearly show that significant overall gains can be achieved by better performance at lower radius. All successful cases have a better overall performance with gains ranging from 25% to 40%. Case H has an excellent overall performance mainly due to the high lift despite a comparatively high drag, as will be shown later. Case A, B and C have a gain close to 27% in spite of a locally worse performance around 70% radius.

From table 1, the local modification property of the b-spline formulation appears to offer some advantage with a gain of over 15% with respect to the number of calls to the RANS solver before reaching the optimum. This is especially true when a surrogate model is used and a higher number of generations are assessed. These results also underline the effectiveness of a GA combined with a surrogate model as in the best case, only 86 calls to the RANS solver are needed. Considering MODE, the results suggest also the effectiveness of using a metamodel as a gain of 23% is obtained globally in that configuration.

The off-design performance of the optimum airfoil is assessed by looking at the airfoil lift coefficient C_l and drag coefficient C_d in successive 2D cascades along the entire blade span. Each radius corresponds to a given angle of attack and Mach number that are different from the optimization ones. This way, transonic to sonic Mach numbers and various angles of attack are ascertained. First, lift-to-drag ratio for all radii are shown in figures 7(a) and 7(b) for the b-spline and Bézier parameterizations respectively. These figures reveal that most of the improvement is achieved at radii below 60% and above 80%. Around 75% radius, there is either a small improvement (cases E and I), no significant improvement (cases A, C, D and H) or even a local deterioration of the performance (case B). From these graphs, the unsatisfactory performance of cases F, G and J is also enlighted.

Case	Optimization method	Levels	Iterations	Calls to RANS solver	Σ-value
	Benchmark				1
A	GA - with ANN - standard b-spline	2	22	258	1.250
B	GA - with ANN - standard Bézier	2	60	372	1.246
C	GA - with ANN - direct b-spline	2	20	252	1.329
D	GA - with ANN - direct Bézier	2	34	294	1.303
E	MODE - with RANS - standard b-spline	1	49	3132	1.302
F	MODE - with RANS - standard Bézier	1	–	6192	0.950
G	MODE - with RANS - direct b-spline	1	–	6192	0.790
H	MODE - with RANS - direct Bézier	1	57	3612	1.408
I	MODE - with ANN - standard b-spline	2	37	2412	1.308
J	MODE - with ANN - standard Bézier	2	–	6192	0.801

Table 1 Cases and number of iterations to optimum solution. (Cases marked with '–' did not converge to an optimum better than the benchmark after 100 iterations.)

Analysis of figures 8(a) and 8(b) reveals that globally all airfoils obtained with b-spline representation perform better than the benchmark. Only case *E* in terms of C_l and cases *A* and *C* in terms of C_d present a shortcoming at a point where they have been optimized (namely 75% radius). But this shortcoming is largely compensated within the trade-off with the other two design points. Additionally, shortcomings at off-design points, as between 58% and 72% radius for C_l or between 68% and 79% for C_d, are overwhelmingly compensated by the global performance out of those intervals. Case *C* denotes himself by the very poor performance in terms of C_d at low radius combined with a terrific value at high radius, hence high Mach number. Together with the exceptional C_l over all radii, this explains why this distorted geometry (see figure 11(b)) made its way through the optimization process. Case *G* is a good example of a failed tentative of local optimization with the drag coefficient having characteristic minima corresponding to the optimization points while the lift coefficient requirement is met at all design points. Concerning Bézier parameterization, figure 9(a) indicates that all airfoils have a favorable behavior in terms of C_l, with the design objective met by all but case *B*. Here again, the overall C_l performance of

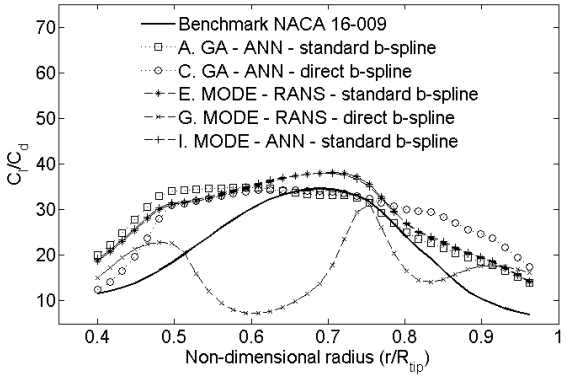

(a) B-spline parameterization.

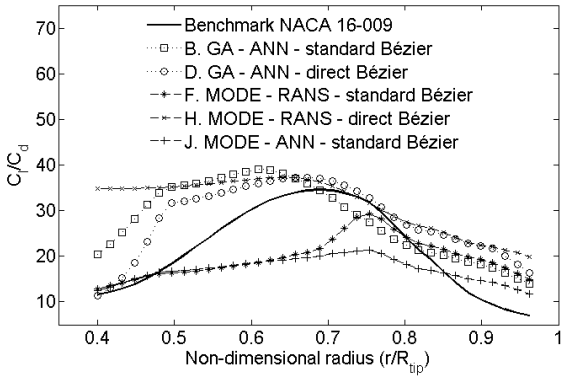

(b) Bézier parameterization.

Fig. 7 Off-design performance in terms of C_l/C_d.

this airfoil largely offsets this minor flaw. As clearly visible from figure 9(b), cases *F* and *J* did not lead to an optimum solution. Despite their overall performance, not a single airfoil is able to achieve lower drag at 75% radius. This is coherent with the observations about the shock strength (see figure 12) that will be given in the coming sections. In any way, the lift-to-drag ratios moderate the local shortcomings discussed here and underline the possibility for additional gains in propeller performance despite possibly lower local performance.

When C_l and C_d distributions are compared in terms of airfoil parameterization, the striking patterns are the better ability of the standard description in producing smooth lift distributions, and the higher potential of b-spline formulation for a drag reduction over the entire range, including off-design points. The first suggests that decomposing the airfoil into a thickness and a camberline distribution introduces a geometrical stiffness in the problem formulation that is beneficial to the lift performance. This complies with the observations made in [16, 24] and [25]. The second underlines the influence of the local modification property. The more direct relationship between the parameters and the shape entitles the optimization process to better identify those design variables that have an influence on lift and drag. The results are better airfoils with a smooth off-design drag distribution provided the intrinsic freedom of the representation is counter-balanced by, for example, the geometrical stiffness of the description. Finally, it is noted that good improvements can be yielded with just a few design variables disregarding the optimization method.

Figures 10(a), 10(b), 11(a) and 11(b) reveal another aspect of the local control property as the shapes obtained with b-spline representation show more local features such as a narrow front section or a bump as on figure 11(a). The first feature is also reported in the work of Li et al [3] although in cases *A*, *E* and *I*, it does not lead to the shock location being moved toward the aft

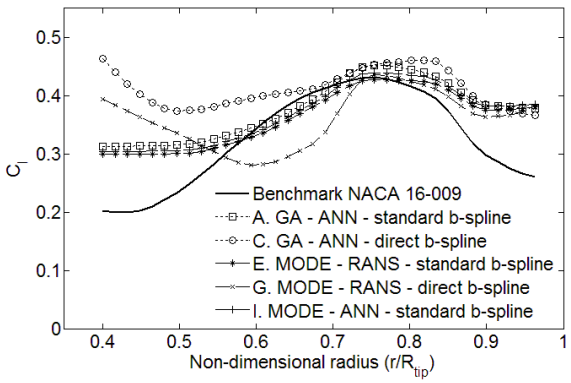

(a) Lift coefficient C_l.

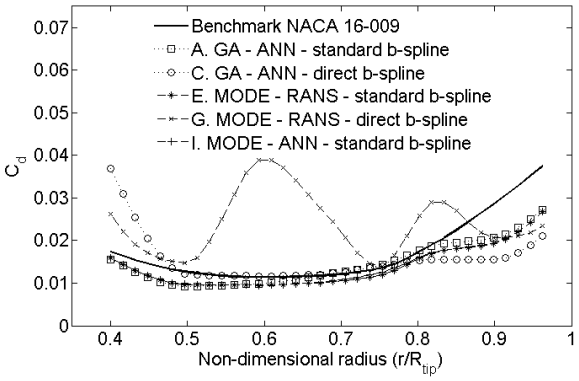

(b) Drag coefficient C_d.

Fig. 8 Off-design performance for b-spline parameterization.

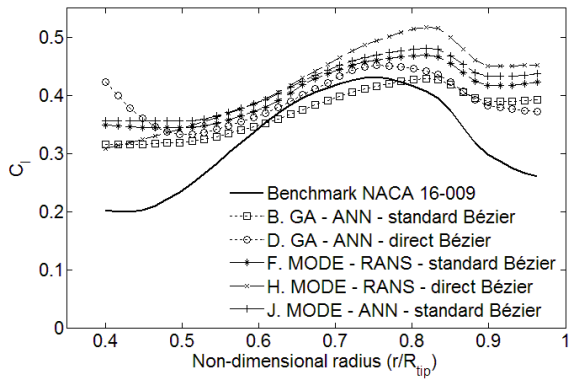

(a) Lift coefficient C_l.

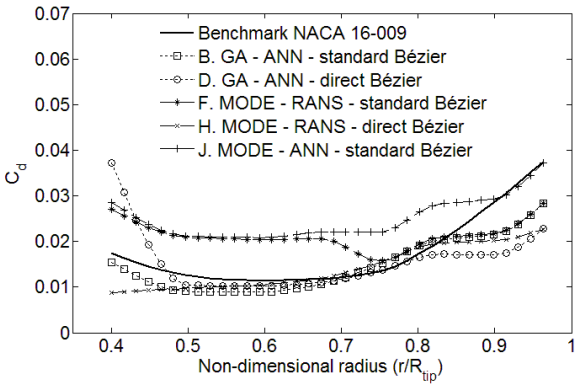

(b) Drag coefficient C_d.

Fig. 9 Off-design performance for Bézier parameterization.

region of the airfoil, as can be seen from the right side of figure 12. The second feature is known to reduce locally the strength of the shock and might lead to localized optimization as discussed by Drela in [33]. Fortunately, the low number of design parameters in the present cases does not allow for bumps to be generated at locations corresponding to each working point. Instead, the geometries are a trade-off and offer shock strength reduction to some extent while retaining the necessary smoothness over the entire chord. In contrast, a Bézier parameterization (see figures 10(a) and 10(b)) does not always lead to a thinner front part (except for case *D*) and is intrinsically impaired of producing local bumps. Accordingly, the shock strength is seldom reduced as is illustrated on the right side of figure 12(a). Except for cases *C* and *G*, all pressure distributions at 75% radius are smooth and present the same general behavior. At 97.5% radius, the pressure distributions reveal that most of the improvement comes from changes on the pressure-side and that schock strength on the suction-side is never reduced in a significant way. A closer study of figure 11(b) reveals the peculiarity of geometries *C* and *G*. Those shapes are the expression of the local control property at its climax because they are not constrained by the intrinsic properties of the formulation nor by the stiffness introduced with the standard description. Case *C* is the best specimen from its parameterization, it successfully meets the design objectives but comes with a high drag at low radius. Case *G* interestingly succeeded in matching some design objectives but, as will be shown later, has poor off-design performance. This underlines the need for some sort of constraints on the regularity of the shape be it by the choice of the formulation or by the choice of the description or ultimately by strong restrictions on the parameters range.

6 Conclusions

The influence of the parameterization and the optimization method on the optimum airfoil is

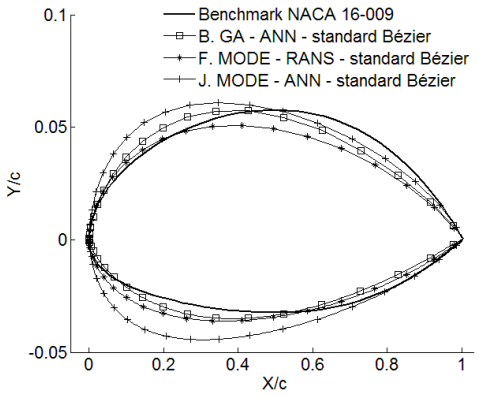

(a) *Standard*.

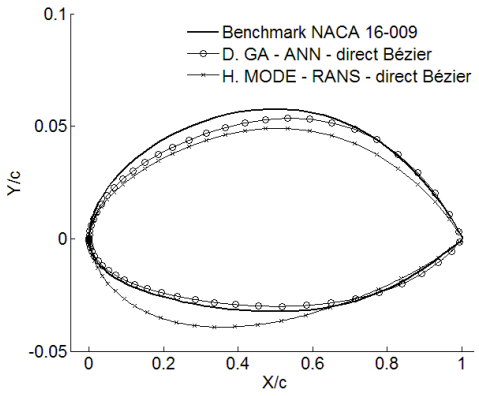

(b) *Direct*.

Fig. 10 Airfoil shapes obtained with the Bézier parameterization.

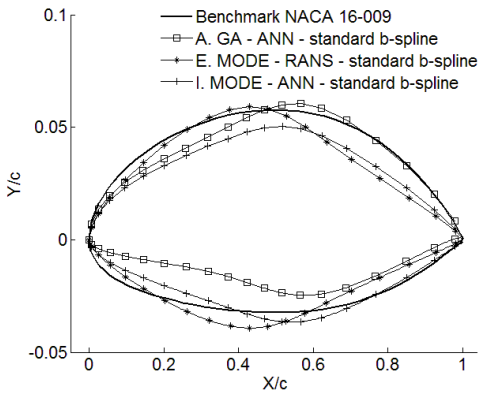

(a) *Standard*.

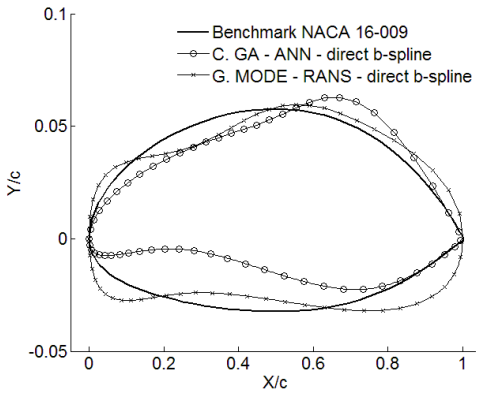

(b) *Direct*.

Fig. 11 Airfoil shapes obtained with the b-spline parameterization.

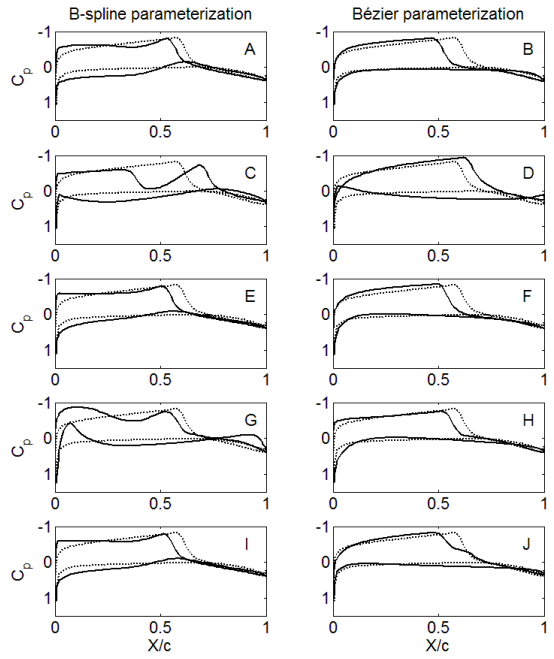

(a) 75% radius.

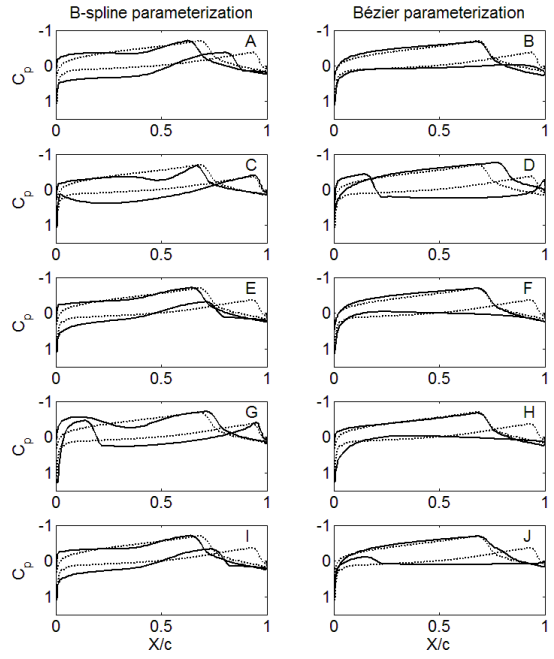

(b) 97.5% radius.

Fig. 12 C_p distributions of the optimum airfoil (' — ' optimum airfoil and '····' benchmark NACA 16-009 airfoil). Non-optimum solutions *F*, *G* and *J* are also shown.

addressed for 10 combinations in the framework of a realistic engineering problem where a sparse amount of variables can be effectively dedicated to the airfoil itself. Standard parameterization using a camberline and thickness distribution outperforms direct parameterization where the airfoil suction- and pressure-sides are directly defined. The latter is true both in terms of aerodynamic performance at design and off-design conditions, and in terms of convergence speed. The results suggest also that b-spline representation globally delivers better aerodynamic results than Bézier formulations. Additionally, b-spline formulations are more efficient in terms of convergence because of the more direct relationship underlying input (the parameters) and output (the shape). The combination of b-spline formulation with the standard thickness-camberline description makes the parameter set more likely to have less interactions and allows it to represent those important features of the design problem that are relevant to lift and drag. This way, the design space is searched more efficiently at some expense of the freedom to generate radically new shapes. Finally, acceleration techniques based on surrogate models offer interesting advantages in terms of computational cost in a population based approach, without significantly affecting the attainable optimum. A requisite for this is to safeguard the accuracy of the metamodel through training in new regions of the search domain with the best individual(s) of a certain number of generations. These issues underline the importance of the choice of the parameterization method on the optimization outcome. Choices regarding parameterization should not be made light-handedly but on the contrary, should be the result of a detailed comparative study that is aimed at the problem to be handled.

Acknowledgments

The author wishes to acknowledge the Belgian Defence Scientific and Technologic Research initiative for its funding of the present study, as well as the von Karman Institute, in particular

R. Van den Braembussche and T. Verstraete, for the resources and expertise made available for the present work.

References

[1] M. Drela and M.B. Giles. Viscous-inviscid analysis of transonic and low Reynolds number airfoils. *AIAA Journal*, 25(10):1347–1355, October 1987.

[2] L. Huyse and R.M. Lewis. Aerodynamic shape optimization of two-dimensional airfoils under uncertain conditions. Contractor Report CR 2001-210648, NASA - ICASE, NASA Langley Research Center (USA), January 2001.

[3] W. Li, L. Huyse, and S. Padula. Robust airfoil optimization to achieve consistent drag reduction over a mach range. Contractor Report CR 2001-211042, NASA - ICASE, NASA Langley Research Center (USA), August 2001.

[4] T. Ray and H.M. Tsai. *Numerical Grid Generation in Computational Field Simulations*, chapter Some issues in NURBS representation of airfoil shapes for optimization, pages 815–825. The International Society of Grid Generation, Mississippi (USA), June 2002.

[5] W. Li and S. Padula. Performance trades study for robust airfoil shape optimization. In *21st AIAA Applied Aerodynamics Conference*, number AIAA 2003-3790, Orlando (USA), June 23-26 2003. AIAA.

[6] M. Nemec and D.W. Zingg. Multipoint and multi-objective aerodynamic shape optimization. *AIAA Journal*, 42(6):1057–1065, June 2004.

[7] M.K. Karakasis, K.C. Giannakoglou, and D.G. Koubogiannis. Aerodynamic design of compressor airfoils using hierarchical, distributed, metamodel-assisted evolutionary algorithms. In *7th European Conference on Turbomachinery, Fluid Dynamics and Thermodynamics*, Athens (Greece), March 5-8 2007.

[8] A.M. Morris, C.B. Allen, and T.C.S. Rendall. CFD-based optimization of aerofoils using radial basis functions for domain element parametrization and mesh deformation. *International Journal for Numerical Methods in Fluids*, 58:827–860, March 2008.

[9] R.A.E. Mäkinen, J. Periaux, and J. Toivanen. Multidisciplinary shape optimization in aerodynamics and electromagnetics using genetic algorithms. *International Journal for Numerical Methods in Fluids*, 30:149–159, 1999.

[10] C. Poloni. *Notes on numerical fluid mechanics*, volume 68, chapter Multi-objective aerodynamic optimisation by means of robust and efficient genetic algorithm, pages 1–24. Vieweg, Wiesbaden (Germany), 1999.

[11] Z.L. Tang and J-A. Désidéri. Towards self-adaptive parametrization of Bézier curves for airfoil aerodynamic design. Research Report INRIA 4572, Institut National de Recherche en Informatique et en Automatique, Sophia Antipolis, September 2002.

[12] S. Peigin and B. Epstein. Robust handling of non-linear constraints for GA optimization of aerodynamic shapes. *International Journal for Numerical Methods in Fluids*, 45:1339–1362, 2004.

[13] S. Peigin and B. Epstein. Robust optimization of 2D airfoils driven by full Navier-Stokes computations. *Journal of Computer and Fluids*, 33:1175–1200, February 2004.

[14] B. Epstein, S. Peigin, and S. Tsach. A new efficient technology of aerodynamic design based on CFD driven optimization. *Aerospace Science and Technology*, 10:100–110, 2006.

[15] D. Lopez, C. Angulo, and L. Macareno. An improved meshing method for shape optimization of aerodynamic profiles using genetic algorithms. *International Journal for Numerical Methods in Fluids*, 56:1383–1389, 2008.

[16] S. Obayashi. Airfoil shape parameterization for evolutionary computation. In *Lecture Series on Genetic Algorithms for Optimisation in Aeronautics and Turbomachinery*, number LS 2000-07, Sint-Genesius-Rode (Belgium), 2000. von Karman Institute for Fluid Dynamics.

[17] J.A. Samareh. Survey of parameterization techniques for high-fidelity multidisciplinary shape optimization. *AIAA Journal*, 39(5):877–884, May 2001.

[18] H-Y. Wu, S. Yang, F. Liu, and H-M. Tsai. Comparison of three geometric representations of airfoils for aerodynamic optimization. In *16th AIAA Computational Fluid Dynamics Con-*

ference, number AIAA 2003-4095, Orlando (USA), June 23-26 2003. AIAA.

[19] W. Song and A.J. Keane. A study of shape parameterisation methods for airfoils optimisation. In *10th AIAA/ISSMO Multidisciplinary Analysis and Optimization Conference*, number AIAA 2004-4482, Albany (USA), August 30 - September 1 2004. AIAA.

[20] S. Obayashi and T. Tsukahara. Comparison of optimization algorithms for aerodynamic shape design. *AIAA Journal*, 35(8):1413–1415, August 1997.

[21] J. Hájek. Parameterization of airfoils and its application in aerodynamic optimization. In *Proceedings of the 16th Annual Conference of Doctoral Students - WDS 2007*, pages 233–240, Prague, June 5-8 2007.

[22] L. Huyse, S.L. Padula, R.M. Lewis, and W. Li. Probabilistic approach to free-form airfoil shape optimization under uncertainty. *AIAA Journal*, 40(9):1764–1772, September 2002.

[23] S. Painchaud-Ouellet, C. Tribes, J.Y. Trépanier, and D. Pelletier. Airfoil shape optimization using a nonuniform rational b-splines parameterization under thickness constraint. *AIAA Journal*, 44(10):2170–2178, October 2006.

[24] I.H. Abbott, A.E. von Doenhoff, and L.S. Stivers Jr. Summary of airfoil data. Report R-824, NACA, NACA-Langley aeronautical laboratory (USA), 1945.

[25] A.J. Keane and P.B. Nair. *Computational approaches for aerospace design*. John Wiley & Sons, Chichester (United Kingdom), 2005.

[26] D. Dasgupta and Z. Michalewicz. *Evolutionary Algorithms - An overview*, chapter Introduction, pages 3–28. Springer-Verlag, Berlin (Germany), 1997.

[27] A. Shahrokhi and A. Jahangirian. Airfoil shape parameterization for optimum navier-stokes design with genetic algorithm. *Aerospace Science and Technology*, 11:443–450, 2007.

[28] D. Goldberg. *Genetic algorithms in search, optimization and machine learning*. Addison-Wesley, Stuttgart (Germany), 1989.

[29] T. Verstraete. *Multidisciplinary turbomachinery component optimization considering performance, stress and internal heat transfer*. Phd thesis, von Karman Institute for Fluid Dynamics - Universiteit Gent, Rhode-Saint-Genèse - Gent (Belgium), June 2008.

[30] K. Price and R. Storn. Differential evolution, April 1 1997.

[31] N.K. Madavan. Multiobjective optimization using a Pareto Differential Evolution Approach. In *Proceedings of the Congress on Evolutionary Computation*, volume 2, pages 1145–1150, Honolulu (USA), 2002.

[32] A. Arnone and R.C. Swanson. A Navier-Stokes solver for turbomachinery applications. *ASME Journal of Turbomachinery*, 115(2):305–313, April 1993.

[33] M. Drela. *Frontiers of Computational Fluid Dynamics*, chapter Pros and cons of airfoil optimization, pages 363–381. World Scientific, Singapore, 1998.

Copyright Statement